Chaos You Can Play In

Aaron Clauset*
Computer Science, University of New Mexico, Albuquerque

Nicky Grigg†
CSIRO, Canberra, Australia

May Lim‡
Physics, University of the Philippines, Diliman

Erin Miller§
Physics, University of Washington, Seattle

September 1, 2003

1 Introduction

Real world instances of complex systems often exhibit complex dynamical behavior that is not well characterized as either *periodic* or *random*. Indeed, many such systems exhibit *chaotic* or *quasi-periodic* behavior. Systems which exhibit chaotic dynamics may be broken into mathematical models, many of which like the *logistic map* or the Lorenz equations are well understood, and real world systems. Chaos in real world systems is significantly more difficult to both model mathematically and explore experimentally. This is due not only to the inherent variability which chaotic behavior creates, but also the inherent difficulties in acquiring good time series measurements. Noise and low sampling rates present problems, as does the fact that there may only be a single stream of data that can be measured in a real system, while in a mathematical model, all variables of interest can be analysed.

Willem Malkus and Lou Howard [1] in the 1970s at MIT improvised the waterwheel, a mechanical analogue of the Lorenz equations. Surprisingly, the waterwheel has remained a largely unexplored system, with what little work has been done focusing on simplifications of the mathematical model [2, 3]. The beauty of the waterwheel is in its simplicity. Water is poured into the system at a steady rate from the top of the tilted wheel. Each cup has a hole drilled in the bottom which allows water to leak out of the system. Some damping is introduced into the rotation of the wheel. By varying only two parameters, the inflow rate of water and friction applied to the wheel, one can cause the wheel to exhibit simple periodic behavior (either unidirectional behavior where the wheel rotates continuously in one direction, or bi-directional behavior in which the wheel reverses direction periodically) or unpredictable transitions between these two simple behaviors. In this paper we describe an experimental and modeling study of the Malkus waterwheel system.

2 Experimental Setup

Our experimental setup (Figure1) consisted of a tilted bicycle wheel with a variable number of removable cups (maximum of $n = 12$ cups) suspended above an underlying pool of water.

*aaron@cs.unm.edu
†Nicky.Grigg@csiro.au
‡may.lim@up.edu.ph
§ebehne@u.washington.edu

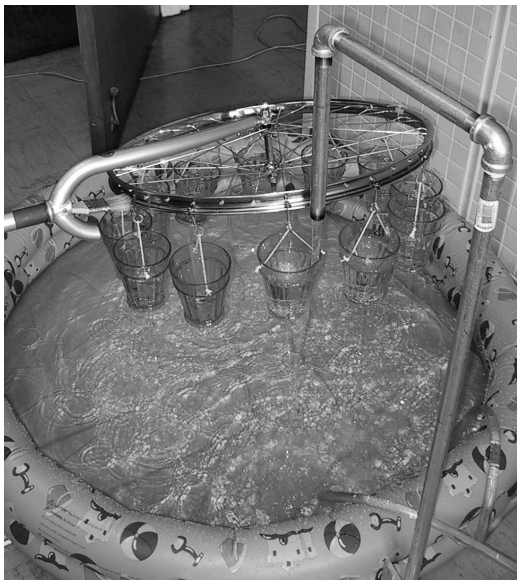

Figure 1: Experimental setup. The apparatus was covered in black for acquiring time series data to in order to optimize the image-tracking software's ability to track the rotation of the wheel.

Table 1: Model parameter values

Parameter	Value	Units	Description
N	12		number of cups
M	0.4	kg	maximum mass in a cup
n	1000		exponent on sin term in Equation 5
r_{leak}	0.0014	m	radius of leak hole in cup
r	0.03325	m	radius of cup
g	9.8	m/s^2	acceleration due to gravity
R	0.25	m	radius of wheel
ρ	998	kg/m^3	density of water
ϕ_0	15	$^\circ$	angle of wheel to horizontal

Water was pumped from the pool to an inflow pipe located at the highest point on the wheel. Apparatus measurements are given in Table 1. A fluorescent ball was mounted on the waterwheel to allow reliable tracking of the wheel's motion [5].

Image tracking software grabbed still-frames of the wheel's state every 500 ms using a color CCD camera mounted with a fish-eye lens. The shutter speed was 1/2000 s to minimize the blurring of the pictures. Object tracking was done in the blue channel where the ball location had a much higher intensity compared to all other pixel elements of the waterwheel setup. The output of the ball-tracking software was a series of (x, y) screen locations. From these screen positions, the angular location θ of the ball were derived. The resultant $\theta(t)$ time series was then interpolated to a finer resolution and numerically differentiated using a second order centered differencing scheme, producing an $\omega(t)$ time series.

3 Governing Equations

The equations of motion for an N-cup Malkus waterwheel can be written, using a Lagrangian description, in terms of $N + 2$ equations. One equation describes the rate of change of one

cup's angular position:

$$\frac{\mathbf{d}\theta_1}{\mathbf{d}t} = \omega \tag{1}$$

Here, θ_1 is the angular position of the first cup and $\theta = 0$ is located at the lowest point of the rotation, opposite the inflow point. The angular positions of the remaining $N-1$ cups are a fixed fraction of 2π from this cup as the angular speed ω is the same for all the cups.

N equations describe the rate of change of mass in each cup. Two terms affect this change for the ith cup; the first term characterizes the rate of mass acquisition as the cup passes under the faucet, while the second describes the rate of mass loss as water continuously drains from the cup:

$$\begin{aligned}\frac{\mathbf{d}m_i}{\mathbf{d}t} = \mathbf{H}\left(M - m_i\right) \cdot Q\Big[\mathbf{H}\left(\theta_i \pmod{2\pi} - \left(\pi - \frac{r}{R}\right)\right) \cdot \\ \mathbf{H}\Big(\left(\pi + \frac{r}{R}\right) - \theta_i \pmod{2\pi}\Big)\Big] - \alpha\sqrt{\frac{2g\rho m_i}{\pi r^2}}\end{aligned} \tag{2}$$

where m_i is the instantaneous mass of the ith cup. The first term describes a flow rate Q, which adds mass to cups with angle $\frac{-r}{R} \leq \theta_i \leq \frac{r}{R}$, where $\mathbf{H}$ represents the Heaviside step function[1]. For simplicity, the function $\left(\sin\left(\frac{\theta_i}{2}\right)\right)^n$ was used in place of the pair of $\mathbf{H}$ functions within Q. This function peaks about $\theta = (2k+1)\pi$ for $k \in \mathbb{Z}$, with a width that narrows as n is increased. We used $n = 1000$ in our simulations. The second term, denoting the leak rate, was derived from Bernoulli's equation, which assumes inviscid laminar flow. Our representation was confirmed experimentally by measuring the drain rate of a cup as it emptied[2]. Finally, the initial step function limits the total mass of liquid in each cup as $m_i \geq M$ results in that cup overflowing.

The rotation of the waterwheel is driven by the nonzero net torque which is a consequence of: the unequal mass distribution around the tilted wheel; the damping applied to the wheel; and the angular momentum gained and lost as mass is transferred into and out of the cup. One equation is needed to describe the rate of change of torque on the wheel:

$$\frac{\mathbf{d}\omega}{\mathbf{d}t}\sum_{i=1}^{N} m_i R^2 + \omega\sum_{i=1}^{N}\frac{\mathbf{d}m_i}{\mathbf{d}t}R^2 = Rg\sin(\phi_0)\sum_{i=1}^{N} m_i \sin\theta_i - \alpha\omega \tag{3}$$

where the first two terms are the angular momentum derivatives - both the angular velocity ω and the moment of inertia I are non-constant functions of time. The right hand side of the equation describes the torques acting on the system due to damping and the mass and location of each cup.

These equations differ from those originally derived for the Malkus waterwheel [1]. Typically, the system is modeled by assuming a continuous ring of water around the wheel (i.e. the limit of infinite cups), where no volume restriction is placed on the cups and leak rate is assumed to be linearly dependent on the mass in a cup. From these assumptions, the equations of motion can be handled analytically, recovering the Lorenz equations through Fourier analysis.

4 Numerical Model

Our numerical simulation of the waterwheel equations offered the following benefits:

1. it provided a method for quantitatively matching our mathematical model of the underlying processes with observable dynamics;

[1]The Heaviside step function is a reasonable approximation to the convolution between the angular width of the cup and that of the water stream from the faucet, given the relative narrowness of the faucet

[2]Although our experimental characterization of the leak-rate was convincing enough for our continued usage of the sublinear term in Equation 2, a more robust characterization would be desirable.

2. it allowed for the more efficient search of parameter space for interesting behavior and thus guide our empirical work;

3. it provided high resolution, noise-free data which facilitated the development and testing of data analysis techniques.

The governing equations were non-dimensionalised to reduce the number of parameters to three dimensionless numbers. The dimensionless variables are

$$m_i^* = \frac{m_i}{M};\ t^* = \frac{t}{T},\ \text{where } T = \sqrt{\frac{R}{g\sin\phi_0}};\ \text{and } \omega^* = \omega T \tag{4}$$

and the non-dimensional equations are

$$\frac{\mathbf{d}m_i^*}{\mathbf{d}t^*} = D_1\sqrt{m_i^*} + D_2\sin^n\left(\frac{\theta_i}{2}\right) \tag{5}$$

$$\frac{\mathbf{d}\omega^*}{\mathbf{d}t^*}\sum_{i=1}^{N} m_i^* + \omega^*\sum_{i=1}^{N}\frac{\mathbf{d}m_i^*}{\mathbf{d}t} = \sum_{i=1}^{N} m_i^*\sin\theta_i - D_3\omega^* \tag{6}$$

$$\frac{d\theta_i}{dt^*} = \omega^* \tag{7}$$

where the dimensionless parameters are:

$$D_1 = \sqrt{\frac{2a^2\rho R}{\pi r^2 M\sin\phi_0}};\ D_2 = \sqrt{\frac{Q^2 R}{Mg\sin\phi_0}};\ \text{and } D_3 = \sqrt{\frac{\alpha^2}{M^2R^3g\sin\phi_0}} \tag{8}$$

These equations were solved numerically using Matlab's ordinary differential equation solver, *ode45*[3]. For $N = 12$ cups, the model consists of fourteen ordinary differential equations: twelve equations to represent the cup masses, one equation for the angular velocity of the wheel and one equation for the cup angular position.

Most simulation parameters could be measured directly from the experimental setup. Although the number and position of the cups could be varied in the experiment and model, we only present results for twelve cups separated uniformly. Generally, only the flow rate Q and the friction applied to the wheel α were varied in simulation and experiment[4]; all other parameters were held constant and are given in Table 1.

Simulations generated time series for each cup's mass $m_i(t)$, the angular velocity of the wheel ω(t) and the angular displacement for a cup $\theta_i(t)$. Further model validation is required; however, our initial comparisons between measurements and model are promising, with good agreement between measured and modelled $\omega(t)$ (Figure 2).

We observed three qualitatively different regimes in $\omega(t)$, determined by the choice of Q and α. We refer to these regimes as *unidirectional*, *regular bi-directional* and *chaotic*. The Q and α values used to illustrate these regimes are given in Table 2, and the corresponding times series $\omega(t)$ and $m_i(t)$ are shown in Figure 3. The angular velocity time series are reminiscent of those generated from the Lorenz equations for periodic and chaotic regimes.

5 Phase Space Reconstruction

Takens' *embedding theorem* gives us a theoretical basis for assuming that we can, with a single time series from our chaotic system, completely reconstruct the phase space of the system dynamics [6, 7]. The embedding theorem does not allow us to reconstruct the original phase space, but rather an equivalent one.

[3]All model results presented here used *ode45*, using the default settings for integration accuracy

[4]In practice, the friction was difficult to vary in a reliable manner and was also held constant for most experimental trials.

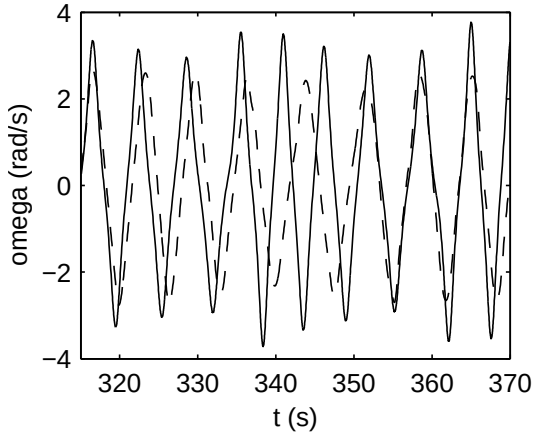

Figure 2: Comparison between modeled (solid line) and measured (dashed line) $\omega(t)$.

Table 2: Parameter values used to illustrate three observed regimes.

Regime name	Q (kg/s)	α (kg m^2/s)
Unidirectional	0.3	0.005
Regular bi-directional	0.11	0.005
Chaotic	0.55	0.04

The phase space reconstruction is done in two parts. One must first determine the *delay coordinate* τ which correctly samples the dynamics of the system. Then one may unfold the attractor from the time series to find the correct *global embedding dimension* d_E. Given τ and d_E, the systems phase space and characteristic attractor may fully reconstructed. We employed the popular *average mutual information* (AMI) algorithm to determine τ and the *false nearest-neighbors* (FNN) algorithm to unfold the attractor and determine d_E [8]. Thus, we chose τ as the first minimum of

$$I(\tau) = \sum_{\omega(t),\omega(t+\tau)} P[\omega(t),\omega(t+\tau)] \log_2 \Big[\frac{P[\omega(t),\omega(t+\tau)]}{P[\omega(t)] \cdot P[\omega(t+\tau)]} \Big] \tag{9}$$

where the angular velocity of the wheel $\omega(t)$ was the time series used for the reconstruction, $P[\omega(t),\omega(t+\tau)]$ is the joint probability of the values $\omega(t)$ and $\omega(t+\tau)$ occurring a time τ apart and $P[\omega(t)]$ is the probability of the value $\omega(t)$ occurring. We selected d_E by choosing the first value of d for which the following *falseness estimator* was below a threshold:

$$\sqrt{\frac{R_{d+1}(t)^2 - R_d(t)^2}{R_d(t)^2}} = \frac{\big|\omega(t+d\tau) - \omega^{NN}(t+d\tau)\big|}{R_d(t)} \tag{10}$$

where

$$R_d(t)^2 = \sum_{m=1}^{d} \big[\omega(t+(m-1)\tau) - \omega^{NN}(t+(m-1)\tau)\big]^2$$

$$R_{d+1}(t)^2 = R_d(t)^2 + \big|\omega(t+d\tau) - \omega^{NN}(t+d\tau)\big|^2$$

We sample the time series $\omega(t)$ in the following manner to reconstruct the phase space, given τ and d_E:

$$\mathbf{y}(t) = \big[\omega(t), \omega(t+\tau), \ldots, \omega(t+(d_E-1)\tau)\big] \tag{11}$$

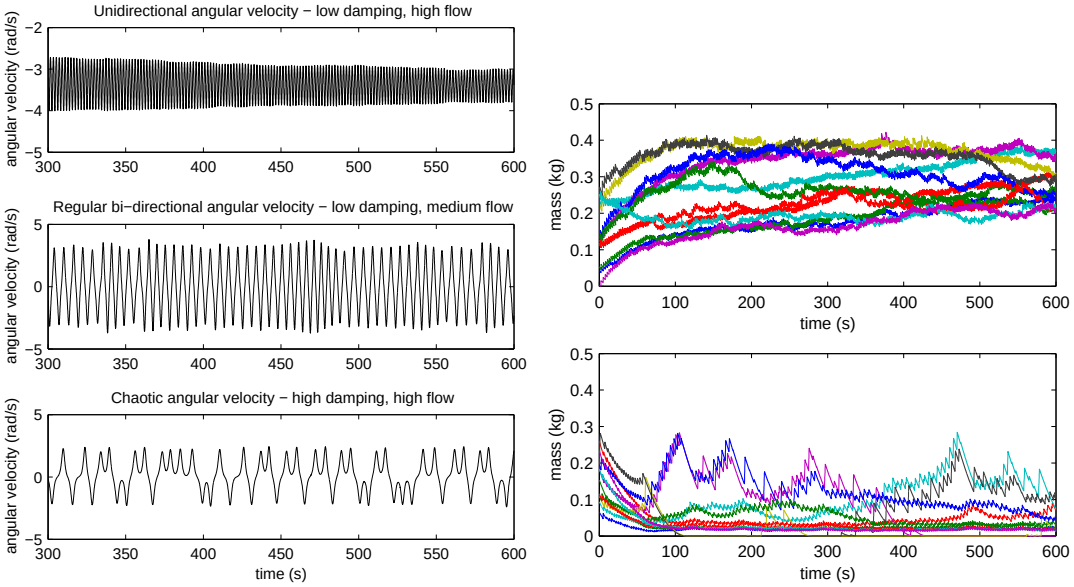

Figure 3: (a) Sample output of $\omega(t)$ for three different regimes. (b) Sample output of water mass in each cup $m_i(t)$ for unidirectional and regular bi-directional regimes.

6 Results

Using the aforementioned algorithms for phase space reconstruction, we reconstructed attractors for numerical data generated by the Lorenz equations and our numerical simulation of the waterwheel to illustrate the strong agreement between the original system of equations and our model. Figure 4 illustrates periodic and chaotic regimes for the Lorenz equations, while Figure 5 illustrates equivalent regions of behavior from the simulation. Further strong agreement was found between the numerical model and empirical data, as shown in . These attractors illustrate the system's transition to chaos behavior, as one can see some degree of complexity in the form of the attractor. From exploring the numerical model, we conjecture that the region of parameter space is large over which the system displays complex but non-chaotic behavior; thus, the waterwheel system may be particularly well suited to for studying the transition between periodic and quasi-periodic regimes.

Although such experiments are extremely difficult to conduct, numerical simulations allow for the exploration of *sensitivity to initial conditions* through local Lyapunov exponents. We observed sensitivity to initial conditions in our model and constructed an animation demonstrating the rapid divergence in reconstructed phase space of two time series with almost identical initial conditions[5] [9]. We leave exact characterization of the Lyapunov exponent for later work.

7 Conclusions

Using the experimental setup, we recorded empirical time series for periodic, quasi-periodic and chaotic waterwheel behavior. We derived the equations of motion for the waterwheel; these equations differ from those usually associated with the waterwheel [1] in that they include more realistic assumptions (discrete number of cups, finite cup volume and more realistic leak rate). These equations were solved numerically and initial comparisons suggest good agreement between empirical and modeled data. Further, applying phase space reconstruction methods to simulated data from the Lorenz and our waterwheel simulation

[5]The initial conditions were differentiated by one gram in one cup.

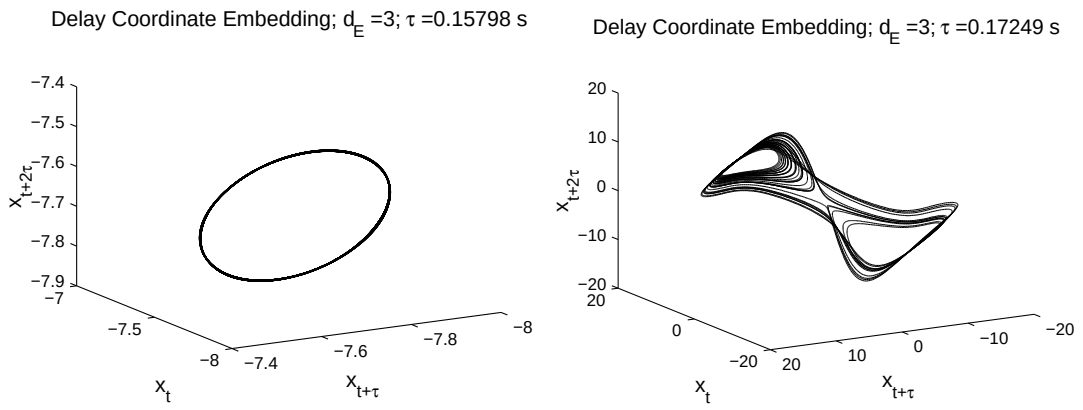

Figure 4: Reconstructed attractors from the periodic (a) and chaotic (b) regimes of the Lorenz equations. (a) $d_E = 3$ and $\tau = 0.1178s$. (b) $d_E = 3$ and $\tau = 0.17295s$.

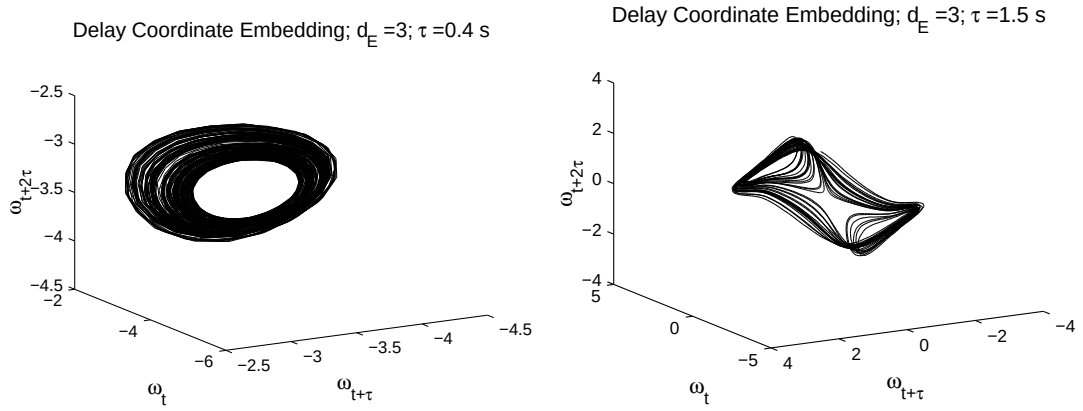

Figure 5: Reconstructed attractors from the periodic (a) and chaotic (b) regimes of the numerical simulation of the waterwheel equations. (a) $d_E = 3$ and $\tau = 0.4s$. (b) $d_3 = 3$ and $\tau = 1.5s$.

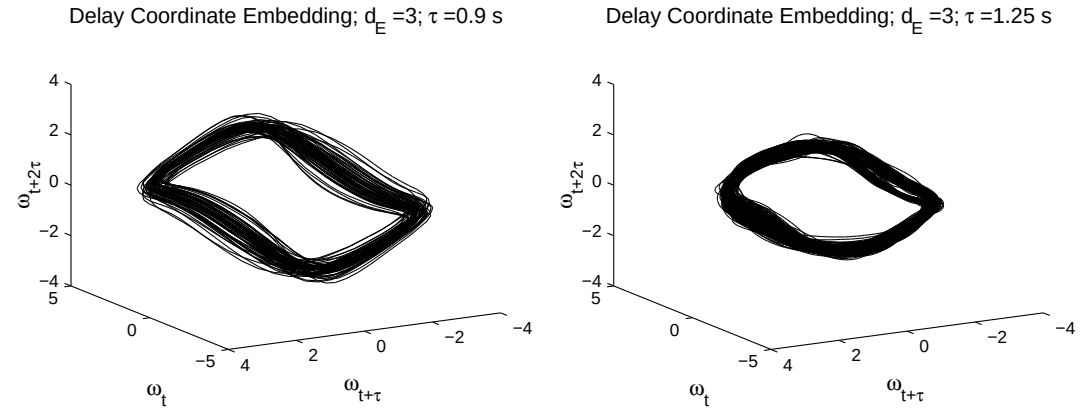

Figure 6: Reconstructed attractors from the near-chaotic regime of the (a) numerical simulation and (b) from empirical data. The numerical simulation was run using parameters taken from the experimental setup which produced (b).

and empirical data revealed a qualitative similarity in the resultant attractors and regimes of behavior. It is left for later work to analyse remaining empirical data[6], calculate the model's Lyapunov exponents and the fractal dimension for model time series.

8 Acknowledgments

Special thanks to Andrew Belmonte and Ray Goldstein for their enthusiastic guidance and invaluable suggestions, to Keith Calamerie for his assistance with the experimental equipment and software, to Tom Carter for his encouragement, enthusiasm and support, and to all those involved in organising the summer school.

References

[1] S. Strogatz. "Nonlinear Dynamics and Chaos." Addison-Wesley, 1994, p. 301-311.

[2] Kolar, M., and Gumbs, G. Theory for the experimental observation of chaos in a rotating wheel. *Phys. Rev. A* 42:626-637, (1992)

[3] Gassmann, F. Noise-induced chaos-order transitions. *Phys. Rev. E*, 55:2215-2221, (1997).

[4] We are grateful to Andrew Belmonte and Penn State University for providing us with a physical waterwheel to utilize in this work. The CSSS waterwheel was built by Bob Geist and Andrew Belmonte from Penn State based on a similar bicycle wheel setup built at Princeton by David Roane and David Wilkinson.

[5] Frame grabbing and tracking software was developed by Ray Goldstein and Keith Calamerie from Univ. of Arizona on NI LabView 6.0 with IMAQ interface.

[6] Takens, F. On the numerical determination of the dimension of an attractor. (1985) In *Lecture notes in mathematics, Vol.1125. Dynamical systems and bifurcations*, Springer, Berlin, p99

[7] Sauer, T., J. A. Yorke, et al. (1991). Embedology. J. Stat. Phys. 65:95-116

[8] Abarbanel, H.D.I. "Analysis of Observed Chaotic Data." Springer Verlag, 1996.

[9] This animation is available in .mov or .avi format from either of the first two authors. See http://cs.unm.edu/∼aaron/waterwheel/movies/

[6] Our additional data includes the time series taken for $N < 12$ cups, which would be particularly interesting if it displays chaotic behavior.